Velocity and attenuation perturbations can hardly be determined simultaneously in acoustic attenuation scattering

W.A. Mulder, Shell International Exploration and Production and Delft University of Technology, and*
B. Hak, Delft University of Technology

SUMMARY

We encountered a fundamental problem in constant-density visco-acoustic imaging of scatterers representing both velocity and attenuation perturbations in the context of seismic exploration with surface data. In the frequency domain, a single complex-valued model parameter that depends on position describes both. Its real part is related to velocity variations, its imaginary part also involves attenuation perturbations. Analysis of the constant-density visco-acoustic wave equation in the Born approximation for a constant background model with horizontally layered scatterers and without density variations shows that recorded surface data hardly change if the scattering model is replaced by a weighted Hilbert transform in depth. Migration of acoustic data for velocity and attenuation perturbations in a known smooth background model reconstructs a linear combination with smallest norm of the true scattering model and its transform. Simultaneous quantitative characterization of velocity and attenuation perturbations will therefore be difficult without additional constraints.

INTRODUCTION

Acoustic imaging of scatterers is a non-invasive method widely used in such diverse fields as medical ultrasound scanning, non-destructive testing, and seismic exploration for oil and gas. Given a known background velocity, the goal is to determine structural information by finding the locations of scatterers in the material. Examples are the outlines of an infant in the womb, cracks in pipelines and concrete, and hydrocarbon bearing geological formations. Qualitative structural images are often sufficient for further interpretation. Quantitative characterization of a scatterer's reflection and attenuation properties may allow for a distinction between, for instance, a cyst and a tumor, a fluid-filled and dry crack, or a fluid-bearing and dry porous rock formation.

We were studying quantitative imaging of geological structures using seismic data in a constant-density acoustic scattering approximation, when we encountered a problem in distinguishing between impedance and attenuation contrasts in the earth. The constant-density assumption reduces impedance contrasts to velocity contrasts. We could determine velocity or attenuation perturbations separately, keeping one of them fixed, but not both simultaneously. Further investigation revealed an ambiguity that did not only occur during imaging, but already at the level of forward modelling, that is, generating synthetic seismic data for the acoustic wave equation in the frequency domain for a given earth model with a finite-difference code. We could show in a 2D numerical example (Mulder and Hak, 2009) that the application of a weighted Hilbert transform in depth to the complex-valued scattering model produces nearly identical data.

To better understand these observations, we simplify the problem to reflections caused by horizontally layered scatterers in an otherwise homogeneous background for a constant-density acoustic wave equation. Pressure data generated by perturbations both in velocity and attenuation are given by the Born approximation and high-frequency asymptotics. We show that a scaled, depth-weighted Hilbert transform of the scatterers provides almost the same data for a choice of parameters that is common in marine seismic exploration. We then derive an expression for the difference between data in the original and the transformed scattering model. This difference is quite small in typical seismic settings. We also show that migration of seismic data will produce a smallest-norm average of the original scattering model and its transform. A numerical experiment for a 2D salt-dome model shows that the same is approximately true in a more complex geological setting.

1D SCATTERER IN A HOMOGENEOUS BACKGROUND

The constant-density visco-acoustic wave equation in the frequency domain is $-\omega^2 \nu \hat{p}_1 - \Delta \hat{p}_1 = s$, where $\hat{p}_1(\omega,\mathbf{x})$ is the pressure, $s(\omega,\mathbf{x})$ a source term, $\omega = 2\pi f$, frequency f, and model parameters

$$\nu(\mathbf{x}) = \frac{1}{v^2} = \frac{1}{c^2}\left[1 - \frac{2}{\pi Q}\log(f/f_r) + \frac{i}{Q}\right].$$

The complex velocity $v(\mathbf{x})$ consists of a sound speed $c(\mathbf{x})$ and quality factor $Q(\mathbf{x})$. Causality dictates the logarithmic term, defined relative to a reference frequency f_r. We split the model into $\nu = \nu_0 + \nu_1$, where ν_0 represents a constant background model and $\nu_1(z)$ a horizontally layered sequence of scatterers that are assumed to be independent of frequency.

For a surface source at $x_s = -h$, $y_s = 0$, $z_s = 0$ with half-offset $h \geq 0$ and a delta function wavelet, the background pressure is given by the Green function $\hat{p}_0(\omega,\mathbf{x}) = (4\pi r_s)^{-1}\exp(ik_0 r_s)$, where $k_0 = \omega/v_0$ and $r_s = [(x+h)^2 + y^2 + z^2]^{1/2}$. The scattered wavefield $\hat{p}_1$ is recorded by a detector or receiver at $x_r = h$, $y_r = 0$, $z_r = 0$. The Born approximation and application of the principle of stationary phase for the integration over x and y leads to

$$\hat{p}_1(\omega,h) \simeq \frac{i\omega c_0}{16\pi}\int_0^\infty e^{2ik_0\sqrt{z^2+h^2}}\,\frac{\nu_1(z)}{z}\,dz. \qquad (1)$$

We assume that $\nu_1(z) = 0$ for $z \leq z_m$, $z_m > 0$.

Our main result is that a scaled and weighted Hilbert transform of the scattering model provides nearly identical data. The Hilbert transform $\mathscr{H}[g]$ of a function $g(z)$, depending on

depth z, is its convolution with $(\pi z)^{-1}$. The scaled and depth-weighted version is the transform

$$\mathscr{M}[g] = -iz\mathscr{H}[g/z]. \qquad (2)$$

The more refined version (Mulder and Hak, 2009) will not be considered here. Although it will improve the results, it will also lengthen the description without changing the basic idea.

Figure 1 shows a simple scattering model $v_1(z)$ and its transform $\mathscr{M}[v_1]$. Parameters are typical for a marine seismic experiment: $c_0 = 1.5\,\mathrm{km/s}$, $f = 15\,\mathrm{Hz}$, $f_r = 1\,\mathrm{Hz}$, and $Q_0 = 100$. The resulting data as a function of half-offset h are displayed in figure 2 and are almost identical after the transform.

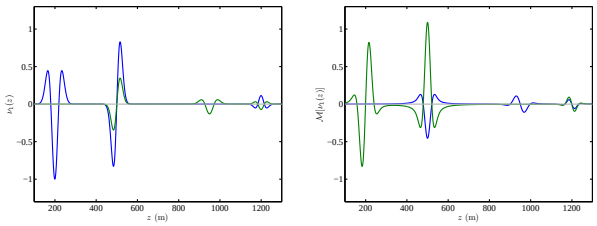

(a) (b)

Figure 1: (a) Scattering model. The blue line represents the real part of the squared slowness perturbation, the green its imaginary part. (b) $\mathscr{M}[v_1]$, its scaled depth-weighted Hilbert transform.

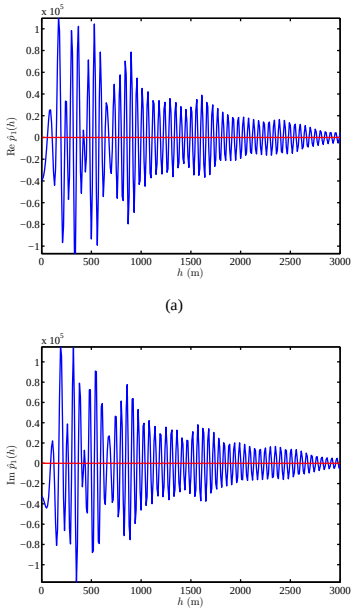

(a) (b)

Figure 2: Real (a) and imaginary part (b) of the recorded pressure at the surface as a function of half the source-receiver distance. The blue line represents the pressure for the original model, the red one the difference between data in the transformed and original model. The difference is too small to be visible.

ANALYSIS

Let $\mu(z) = v_1(z)/z$. For fixed half-offset h and angular frequency ω, the pressure data are

$$\hat{p}_1 = A\int_{-\infty}^{\infty} f_1(z)\mu(z)dz, \quad f_1(z) = e^{2ik_0\sqrt{h^2+z^2}}H(z), \qquad (3)$$

where $H(z)$ denotes the Heaviside or unit step function. The data for the transformed model are given by $-iA\int_{-\infty}^{\infty} f_1\mathscr{H}[\mu]dz = iA\int_{-\infty}^{\infty}\mathscr{H}[f_1]\mu\,dz$. To find a relation between f_1 and $\mathscr{H}[f_1]$, we consider a contour in the first quadrant of the complex plane bounded by the positive real and positive imaginary axis. We want to determine the integral

$$\mathscr{J}_1(z) = \mathscr{H}[f_1] = \frac{1}{\pi}\int_{-\infty}^{\infty}\frac{f_1(x)}{z-x}dx.$$

If $z > 0$, we have a pole on the real axis which, when passed by a semi-circle from above, results in a contribution $\mathscr{J}_2 = if_1(z)$ by the residue theorem. Next, we follow a quarter of a circle from the positive real axis to the positive imaginary axis with a radius that goes to infinity. This contributes $\mathscr{J}_3 = 0$. Finally, we have to integrate over the positive imaginary axis:

$$\mathscr{J}_4 = \frac{i}{\pi}\int_{\infty}^{0}\frac{f_1(iy)}{z-iy}dy = -i\left[f_2(z)+f_3(z)\right],$$

with

$$f_2(z) = \frac{i}{\pi}\int_0^1\frac{e^{i\alpha\sqrt{1-\xi^2}}}{\xi+i\tilde{z}}d\xi, \;\; f_3(z) = \frac{i}{\pi}\int_1^{\infty}\frac{e^{-\alpha\sqrt{\xi^2-1}}}{\xi+i\tilde{z}}d\xi.$$

Here $\alpha = 2hk_0$ and $\tilde{z} = z/h$. From $\mathscr{J}_1+\mathscr{J}_2+\mathscr{J}_3+\mathscr{J}_4 = 0$, we obtain $f_1 = i\mathscr{H}[f_1]+f_2+f_3$. The difference between the data in the transformed and the original model is $-A\int_{-\infty}^{\infty}(f_2+f_3)\mu dz$.

There are two reasons why this difference can be small, relative to the data in the original model. First, f_1 is an oscillatory function of z, whereas f_2 and f_3 are smooth. If the scatterers v_1 are obtained as the difference between a rough earth model v and its smoothed version v_0, they have an oscillatory character. Their interaction with f_1 will produce a large contribution relative to the smoothing effect of f_2 and f_3. Secondly, f_2 and f_3 are smaller than f_1 for typical parameter choices. We can derive the following bounds: $|f_1| \le \exp(-\mathrm{Im}\,(\alpha)\sqrt{1+\tilde{z}^2})$, $|f_2| \le (1/\pi)\,\mathrm{arcsinh}\,(1/|\tilde{z}|)$, and $|f_3| \le 1/(\pi|\alpha|^2\sqrt{1+\tilde{z}^2})$. The bound for f_2 is not very sharp. For small $\tilde{z}$, f_2 has a logarithmic singularity where $|f_2|$ will exceed $|f_1|$.

Marine surveys typically have offsets ($2h$) between 125 m and 3 to 12 km for targets down to a depth of about half the maximum offset. Recording times between successive shots are about 5 to 10 seconds. Seismic data are usually band-limited to the range between, roughly, 10 and 100 Hz. Reflections from larger depths are weaker because of attenuation and geometrical spreading – the factor $1/z$ in equation (1) – and will drop below the noise level at some point, making longer recording times unnecessary.

Figure 3 compares the magnitudes of f_1, f_2, and f_3 for the same parameters as before at half-offsets of 50 and 1000 m.

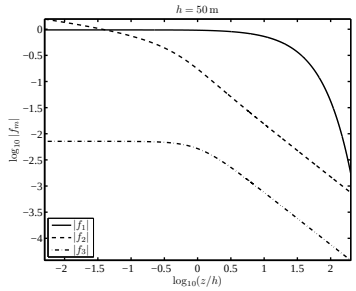

(a)

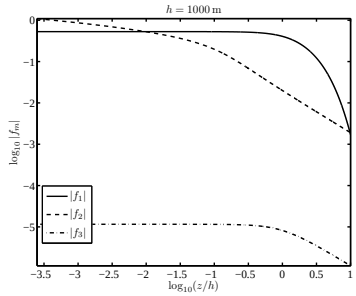

(b)

Figure 3: Comparison of the f_1 (solid), f_2 (dashed), and f_3 (dash-dot) for a half-offset of 50 m (left) and 1000 m (right).

Clearly, $|f_3| \ll |f_2|$ and $|f_2|$ lies well below f_1 in the range where $z/h = O(1)$. This is consistent with the earlier result that almost the same data are found for the original and transformed model. Differences arise at small and large depths. At smaller depths, the logarithmic singularity in f_2 shows up. At larger depths, $|f_1|$ drops below $|f_2|$ due to the attenuation of the background medium. The latter causes the exponential decay of f_1, whereas f_2 decreases as $1/z$.

The fact that f_1 dominates over $f_2 + f_3$ does not necessarily imply that the integration with μ in equation (3) will produce a larger result for f_1. If, for instance, μ is constant over a range of depths, the oscillatory behavior of f_1 will cause cancellation in the integration. The smoother functions f_2 and f_3 may then produce a larger result after integration. We studied this behavior by applying a Fourier transform in depth and found that the small wavenumbers, or long wavelengths, of μ will lead to large contributions for f_2 and f_3 after integration, relative to f_1. Therefore, we only obtain approximately the same pressure data for the scattering model v_1 and its transform $\mathscr{M}[v_1]$ if the model is sufficiently oscillatory in depth. This is the case in the example of figure 1. Because, in practice, the scattering model can be defined as the difference between the original rough model and its smooth version, it will be oscillatory by construction. The smooth version should produce kinematically correct wavefields without significant reflections in the seismic frequency bandwidth.

We conclude that surface data for a sufficiently oscillatory scattering model at not too shallow depths hardly change after a scaled and weighted Hilbert transform in depth. As a consequence, quantitative simultaneous imaging of velocity and attenuation perturbations will be nearly impossible. Note that, in practice, the fact that $Q \gg 1$ for frequencies in the seismic band by itself makes it difficult to measure scattering attenuation effects. The ambiguity described here only makes it worse. The next question is: what kind of scattering model will migration actually provide?

MIGRATION

The goal of linearized inverse scattering is the reconstruction of both the geometry and the intrinsic properties of the scatterers. Mathematically, the inverse problem can be posed as minimization of the least-squares error between modelled and observed data. If the initial model is smooth, it will hardly produce reflections in the frequency-band of the observations. The direct wave from source to receivers is usually removed from the data. As a result, the data difference for the first iteration will equal the pre-processed data. The gradient of the error cost function with respect to the model parameters for this first iteration will provide a subsurface image. Given the substantial computational cost of this procedure, the inversion process is usually stopped after a single iteration. The image provides structural information about the scatterers. With proper weighting, quantitative information can be extracted. The pseudo-inverse of the Hessian of the cost function provides the best weighting, because it solves the least-squares problem in a single step. Since the Hessian is usually too costly to compute, a suitable diagonal approximation is often used. With these so-called migration weights, one or a few iterations usually suffice to obtain quantitative 'true-amplitude' results in the absence of attenuation (Beylkin, 1985; Docherty, 1991; ten Kroode et al., 1994; Chavent and Plessix, 1999; Gray, 1997; Shin et al., 2001; Østmo et al., 2002; Plessix and Mulder, 2004; Mulder and Plessix, 2004a). Consider the least-squares error $\sum_{h,\omega} |\hat{p}_1^{\rm obs}(\omega,h) - \hat{p}_1(\omega,h)|^2$, where $\hat{p}_1^{\rm obs}$ are observed and $\hat{p}_1 = F v_1$ modelled data for receivers located at a finite number of offsets. The linear operator F is defined by equation (1). The inverse problem requires the solution of $F^{\rm H} F v_1 = F^{\rm H} \hat{p}_1^{\rm obs}$. Here $F^{\rm H}$ denotes the conjugate transpose of F. The Hessian $F^{\rm H} F$ is singular or close to singular, as follows from the earlier discussion.

After preprocessing of the data to remove the factor $i\omega$ and the source signature over the available frequency range, we obtain the weighted migration image

$$m(z_1) \propto z_1 \sum_h \int_{\omega_{\rm min}}^{\omega_{\rm max}} d\omega \int_0^\infty dz_2 \, e^{2i(k_0 r_2 - k_0^* r_1)} v_1(z_2)/z_2,$$

where $r_k = \sqrt{z_k^2 + h^2}$ for $k = 1, 2$ and the asterisk denotes the complex conjugate. Its weighted Hilbert transform, $\mathscr{H}[m(z_1)/z_1]$, involves $\mathscr{H}[f_1^*]$. Therefore, $\mathscr{H}[m(z_1)/z_1] \simeq i(m(z_1)/z_1)$.

The last result represents a minimum-norm solution in the following sense. Since μ and $-i\mathscr{H}[\mu]$ approximately produce the same data, a linear combination of the form $(1-\gamma)\mu + \gamma(-i\mathscr{H}[\mu])$ will do that as well. It is straight-forward to show that the smallest norm is obtained for $\gamma = \frac{1}{2}$. The result has the property $\mathscr{H}\left[\frac{1}{2}(\mu - i\mathscr{H}[\mu])\right] = i\frac{1}{2}(\mu - i\mathscr{H}[\mu])$. Because

m/z has the same property, we have shown that weighted linearized inversion or migration produces a reconstruction of $\frac{1}{2}(\mu - i\mathscr{H}[\mu])$. The limited frequency range implies that the reconstruction will be band-limited.

MIGRATION IN A 2D EXAMPLE

Earlier (Mulder and Hak, 2009), we found that the ambiguity occurred in a 2D constant-density visco-acoustic model. Here, we investigate the migration image obtained for the data generated in that example. Figure 4 shows a blocky salt-dome model, which was replaced by a smooth version. We took the difference of the complex-valued squared slowness between the original and smoothed model as a scattering model and solved the pair of wave equations that represents the Born approximation. The resulting data only contained primary reflections. It turned out that a weighted Hilbert transform in depth of the scattering model produces nearly the same data if the reflectors were not too shallow and not too steeply dipped. This agrees with the conclusions obtained in the 1D case.

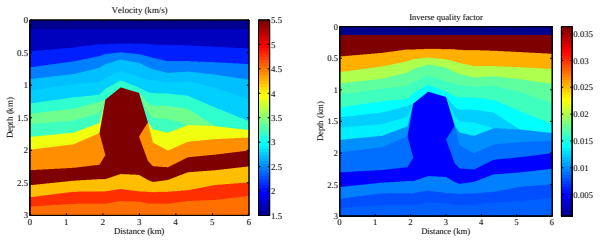

(a) (b)

Figure 4: Original model with velocity c (left) and inverse quality factor $1/Q$ (right).

We performed true-amplitude migration (Plessix and Mulder, 2004; Mulder and Plessix, 2004a,b) of the synthetic data in the smooth background model. Figure 5 displays vertical cross sections taken from the 2D migration images. In the 2D case, we have to modify the geometrical spreading factor in the depth-weighted Hilbert transform $\mathscr{M}[\cdot]$ of equation 2: instead of z, we use $\sqrt{z}$. The result of applying this transform to the migration result is shown by the red lines in figures 5(a) and 5(b). The migration result and its transform match quite well, except for the shallow reflectors and the deeper part around 1.5 km depth, where the steeply dipping salt flank is located. This demonstrates that the minimum-norm solution of the previous section is also obtained in the 2D case for not too shallow and not too strongly dipped reflectors.

DISCUSSION

We have shown that two different oscillatory scattering models provide almost identical data and that migration produces a scattering model that is a weighted average of the two with smallest norm. This implies that it is impossible to uniquely determine both the velocity and attenuation perturbations from the data without additional constraints. The transformed model,

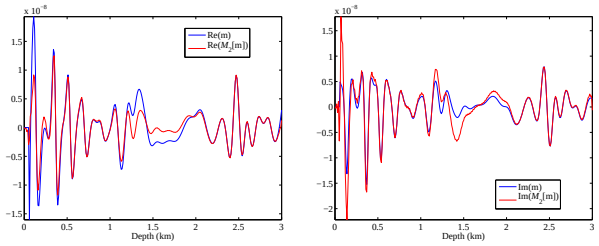

(a) (b)

Figure 5: Cross sections of the migration image at 2 km distance from the origin. The blue line represents the result for the original model, the red line for the transformed one. The real part is shown on the left, the imaginary part on the right.

for instance, when added to the background model, may correspond to unphysical values of the perturbed attenuation, both in size and sign. Suitable constraints on admissible solution will reduce, but possibly not remove, the ambiguity.

Our result seems to contradict conclusions on visco-acoustic inversion by several authors, so some comments are in place. Some authors (Ribodetti et al., 1995; Ribodetti and Virieux, 1998; Innanen and Weglein, 2007; Hak and Mulder, 2008) consider point scatterers of delta-function type or blocky perturbations. Because these contain long wavelengths, they do not fit our assumption of a sufficiently oscillatory scattering model. Another way to understand this, is the fact that their Hilbert transform is proportional to inverse depth, so the transformed model will produce near-surface scattering even if the scatterer itself is buried at large depth. Clearly, our observed ambiguity will not occur in that case and linearized inversion should be feasible. Density, velocity, and attenuation perturbations can be recovered by inversion if only one of these parameters at the time is considered (Blanch and Symes, 1994; Ribodetti et al., 1995). With the constraint that the inverted parameter is either real or imaginary, the ambiguity is removed.

We should emphasize that our observations do not relate to attenuation estimates from diving waves or direct arrivals in crosswell or surface-to-well transmission data. These provide a characterization of the background model. For scatterers that represent the difference between a rough earth model and its smoothed version, which should be kinematically correct without producing significant reflections in the seismic frequency range, the ambiguity will occur for not too shallow reflectors with small dips. A more detailed description will be published elsewhere (Mulder and Hak, Geophysical Journal International).

ACKNOWLEDGMENTS

This work is part of the research programme of the 'Stichting voor Fundamenteel Onderzoek der Materie (FOM)', financially supported by the 'Nederlandse Organisatie voor Wetenschappelijk Onderzoek (NWO)' and by 'Stichting Shell Research'.

EDITED REFERENCES

Note: This reference list is a copy-edited version of the reference list submitted by the author. Reference lists for the 2009 SEG Technical Program Expanded Abstracts have been copy edited so that references provided with the online metadata for each paper will achieve a high degree of linking to cited sources that appear on the Web.

REFERENCES

Beylkin, G., 1985, Imaging of discontinuities in the inverse scattering problem by inversion of a causal generalized Radon transform: Journal of Mathematical Physics, **26**, 99–108.

Blanch, J. O., and W. W. Symes, 1994, Linear inversion in layered viscoacoustic media using a time-domain method: 64th Annual International Meeting, SEG, Expanded Abstracts, 1053–1056.

Chavent, G., and R. É. Plessix, 1999, An optimal true-amplitude least-squares prestack depth-migration operator: Geophysics, **64**, 508–515.

Docherty, P., 1991, A brief comparison of some Kirchhoff integral formula for migration and inversion: Geophysics, **56**, 1164–1169.

Gray, S., 1997, True amplitude migration: A comparison of three approaches: Geophysics, **62**, 929–936.

Hak, B., and W. A. Mulder, 2008, Preconditioning for linearised inversion of attenuation and velocity perturbations: 70th Annual Conference and Exhibition, EAGE, Extended Abstracts, H002.

Innanen, K. A., and A. B. Weglein, 2007, On the construction of an absorptive-dispersive medium model via direct linear inversion of reflected seismic primaries: Inverse Problems, **23**, 2289–2310.

Mulder, W. A., and B. Hak, 2009, Simultaneous imaging of velocity and attenuation perturbations from seismic data is nearly impossible: 71st Annual Conference and Exhibition, EAGE, Extended Abstracts, S043.

Mulder, W. A., and R. É. Plessix, 2004a, A comparison between one-way and two-way wave-equation migration: Geophysics, **69**, 1491–1504.

Mulder, W. A., and R. É. Plessix, 2004b, How to choose a subset of frequencies in frequency-domain finite-difference migration: Geophysical Journal International, **158**, 801–812.

Østmo, S., W. A. Mulder, and R. É. Plessix, 2002, Finite-difference iterative migration by linearized waveform inversion in the frequency domain: 72nd Annual International Meeting, SEG, Expanded Abstracts, **21**, 1384–1387.

Plessix, R. É., and W. A. Mulder, 2004, Frequency-domain finite-difference amplitude-preserving migration: Geophysical Journal International, 157, 975–987.

Ribodetti, A., and J. Virieux, 1998, Asymptotic theory for imaging the attenuation factor Q: Geophysics, **63**, 1767–1778.

Ribodetti, A., J. Virieux, and S. Durand, 1995, Asymptotic theory for viscoacoustic seismic imaging: 65 th Annual International Meeting, SEG, Expanded Abstracts, 631–634.

Shin, C., S. Jang, and D. J. Min, 2001, Improved amplitude preservation for prestack depth migration by inverse scattering theory: Geophysical Prospecting, **49**, 592–606.

ten Kroode, A. P. E., D. J. Smit, and A. R. Verdel, 1994, A microlocal analysis of migration: Wave Motion, **28**, 149–172.